

Article

Application of POCOP Pincer Nickel Complexes to the Catalytic Hydroboration of Carbon Dioxide

Jie Zhang *, Jiarui Chang, Ting Liu, Bula Cao, Yazhou Ding and Xuenian Chen *

School of Chemistry and Chemical Engineering, Henan Key Laboratory of Boron Chemistry and Advanced Energy Materials, Henan Normal University, Xinxiang 453007, China; changjiaruicjr@163.com (J.C.); liuting_233@163.com (T.L.); bulacao@126.com (B.C.); yazhouding_1@163.com (Y.D.)

* Correspondence: jie.zhang@htu.edu.cn (J.Z.); xnchen@htu.edu.cn (X.C.); Tel.: +86-373-332-8655 (J.Z. & X.C.)

Received: 1 October 2018; Accepted: 29 October 2018; Published: 1 November 2018



Abstract: The reduction of CO₂ is of great importance. In this paper, different types of bis(phosphinite) (POCOP) pincer nickel complexes, [2,6-(R₂PO)₂C₆H₃]NiX (R = ^tBu, ⁱPr, Ph; X = SH, N₃, NCS), were applied to the catalytic hydroboration of CO₂ with catecholborane (HBcat). It was found that pincer complexes with ^tBu₂P or ⁱPr₂P phosphine arms are active catalysts for this reaction in which CO₂ was successfully reduced to a methanol derivative (CH₃OBcat) with a maximum turnover frequency of 1908 h⁻¹ at room temperature under an atmospheric pressure of CO₂. However, complexes with phenyl-substituted phosphine arms failed to catalyze this reaction—the catalysts decomposed under the catalytic conditions. Complexes with ⁱPr₂P phosphine arms are more active catalysts compared with the corresponding complexes with ^tBu₂P phosphine arms. For complexes with the same phosphine arms, the catalytic activity follows the series of mercapto complex (X = SH) ≈ azido complex (X = N₃) >> isothiocyanato complex (X = NCS). It is believed that all of these catalytic active complexes are catalyst precursors which generate the nickel hydride complex [2,6-(R₂PO)₂C₆H₃]NiH in situ, and the nickel hydride complex is the active species to catalyze this reaction.

Keywords: nickel catalyst; hydroboration; carbon dioxide; catecholborane; pincer complex; mercapto complex; azido complex; isothiocyanato complex

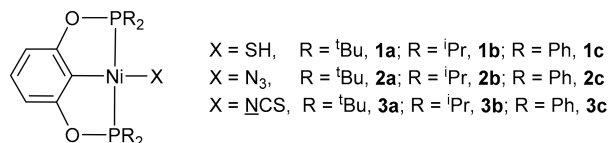
1. Introduction

The development of effective chemical processes that catalytically convert carbon dioxide to valuable compounds has received a great deal of attention recently [1–6]. Of the various chemical transformations investigated, catalytic reduction of CO₂ to methanol (MeOH) is of particular interest because the latter is a very important commodity chemical and can be used as a type of clean fuel. Over the last 20 years, great efforts have been made to reduce CO₂ to MeOH or its derivatives [5–13]. Specifically, significant progress or breakthroughs have been achieved in metal catalyzed homogeneous conversion of CO₂ to MeOH [14–29].

As an earth-abundant cost-effective late transition metal, nickel has been extensively used to catalyze a variety of chemical transformations since the last century. Nowadays, homogeneous nickel catalysis is becoming more and more important in modern synthetic chemistry because of the diverse novel catalytic reactivities of nickel complexes [30–32].

We have been interested in the chemistry of transition metal complexes bearing bis(phosphinite) (POCOP) pincer ligands [14,15,26,27,33–38]. Recently, we applied some POCOP pincer nickel thiolato complexes, [2,6-(R₂PO)₂C₆H₃]NiY (R = ^tBu, ⁱPr; Y = SC₆H₄-*p*-OCH₃, SC₆H₄-*p*-CH₃, SPh, SC₆H₄-*p*-CF₃, SCH₂Ph), to the catalytic reduction of CO₂ with catecholborane (HBcat) [27]. Carbon dioxide was effectively reduced to CH₃OBcat under very mild conditions, and turnover frequencies (TOFs) up

to 2400 h^{-1} were observed. Although POCOP pincer nickel hydrides are also good catalysts for this reaction under the same conditions [14–16], the catalytic activity of the nickel thiolato complexes are better than that of the corresponding nickel hydride complexes. It was concluded that the thiolato complexes may work as pre-catalysts with the *in situ* generated nickel hydride complexes being the real active species. The superior catalytic activity of the thiolato complexes may be due to some *in situ* generated thiolato species that act as co-catalysts. To confirm this speculation, we initiated a more extensive study for this hydroboration reaction. In this paper, we used different types of POCOP pincer ligated nickel complexes with different phosphine arms and different auxiliary ligands, $[2,6-(R_2PO)_2C_6H_3]NiX$ (Scheme 1), to catalyze this reaction under the same conditions. It was found that pincer complexes with tBu_2P or iPr_2P arms are active catalysts and CO_2 was reduced to CH_3OBcat at room temperature under an atmospheric pressure of CO_2 . Turnover frequencies up to 1908 h^{-1} were observed. Complexes with iPr_2P arms are more active catalysts compared with the corresponding complexes with tBu_2P arms. For complexes with the same phosphine arms, the catalytic activity follows the series of mercapto complex ($X = SH$) \approx azido complex ($X = N_3$) $>>$ isothiocyanato complex ($X = NCS$). The results are consistent with the speculation that these different types of pincer nickel complexes are catalyst precursors and the *in situ* generated pincer nickel hydrides are the actual active species to catalyze the hydroboration of carbon dioxide with catecholborane.

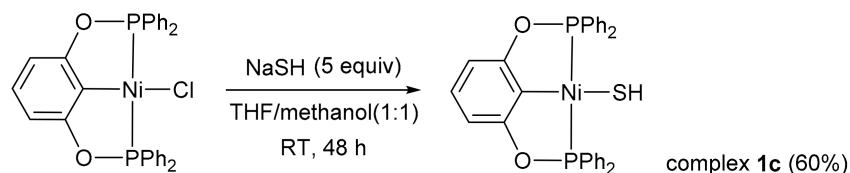


Scheme 1. The nickel complexes used for the catalytic hydroboration of CO_2 with $HBcat$.

2. Results and Discussion

2.1. Synthesis and Characterization of the Ni Catalysts

Complexes **1a** [37], **1b** [38], **2a–c** [35] and **3a–c** [35] were synthesized as described in the literatures. Complex **1c** has never been reported before and was synthesized by the reaction between $[2,6-(Ph_2PO)_2C_6H_3]NiCl$ and $NaSH$ in THF/methanol at room temperature (Scheme 2). As a new complex, **1c** was fully characterized by nuclear magnetic resonance spectroscopy (NMR), Fourier Transform infrared spectroscopy (FTIR), X-ray crystallography and elemental analysis.



Scheme 2. Synthesis of complex **1c**.

Complex **1c** is an air-sensitive orange solid and is soluble in toluene and dichloromethane. The 1H , $^{13}C\{^1H\}$ and $^{31}P\{^1H\}$ NMR spectra of **1c** were in good agreement with the structure depicted in Scheme 2. Complex **1c** showed the expected spectra characteristics for a POCOP pincer ligated nickel complex [14–16,27,33–42]. Similar to other reported transition metal mercapto complexes [37,38,43–45], the 1H NMR resonance of the $-SH$ proton of **1c** appeared in a relatively high-field (-0.76 ppm) as a triplet. An H-P coupling constant of 19.7 Hz was observed. The $^{31}P\{^1H\}$ NMR spectrum of **1c** displayed one singlet, implying an identical chemical environment for the two phosphine arms in solutions. The FTIR spectrum of **1c** displayed a weak absorption at 2546 cm^{-1} which was attributed to the S-H stretching vibration.

Single crystals of **1c** used for X-ray diffraction analysis were obtained by recrystallization in *n*-hexane/CH₂Cl₂ solution at −10 °C. The identity of the crystals was affirmed by ³¹P{¹H} NMR spectroscopy. The diffraction experiment was carried out at 103 K using a Bruker SMART6000 CCD diffractometer (Bruker Corporation, Karlsruhe, Germany). The molecular structure of **1c** is shown in Figure 1 and the selected bond lengths and angles are also provided.

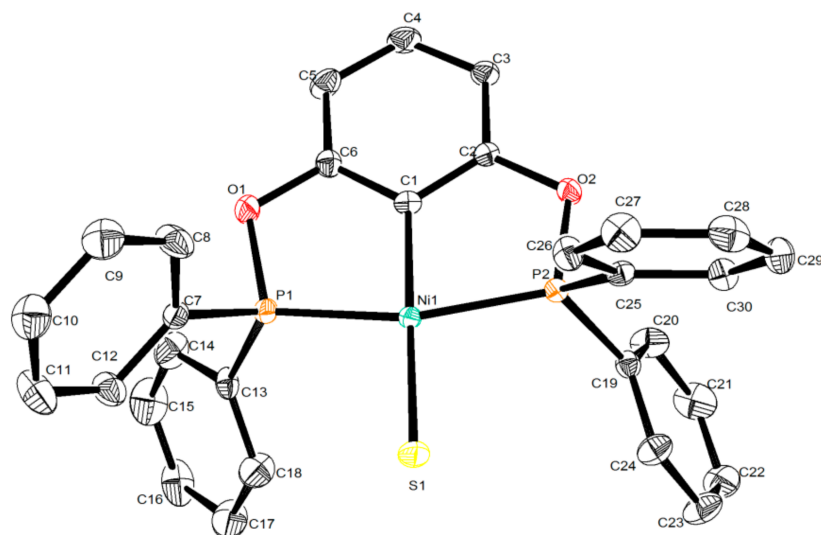


Figure 1. Thermal ellipsoid plots of complex **1c** at the 50% probability level (hydrogen atoms are omitted for clarity). Selected bond lengths (Å) and angles (deg): Ni1–C1, 1.890(2); Ni1–P1, 2.1389(8); Ni1–P2, 2.1456(8); Ni1–S1, 2.1852(7); P1–Ni1–P2, 164.13(3); S1–Ni1–C1, 177.33(8); P1–Ni1–S1, 98.78(3); P2–Ni1–S1, 97.00(3).

As shown in Figure 1, the square-planar geometry for the Ni center of **1c** is distorted; this is quite common for POCOP pincer nickel complexes [14–16,27,33–42]. Both the C_{ipso}–Ni and Ni–S bond lengths in complex **1c** are comparable to those of the related pincer nickel mercapto complexes with ^tBu₂P or ⁱPr₂P arms [37,38]. This indicates that the C_{ipso}–Ni and Ni–S bond strengths are not considerably affected by the substituents on the phosphine arms.

2.2. Catalytic Hydroboration of CO₂ with HBcat

In order to check the catalytic activities, a NMR tube reaction was carried out for each of the nickel complexes. Typically, the nickel complex (0.01 mmol) was mixed with HBcat (0.3 mmol) in C₆D₆ (0.5 mL) in a NMR tube under a N₂ atmosphere. Carbon dioxide was then introduced and the reaction was monitored by NMR spectra at room temperature. For complexes **1a**, **1b**, **2a**, **2b** and **3b**, the ¹¹B NMR spectra showed that HBcat was completely or partly consumed in 30 min. CH₃OBcat and catBOBcat were formed as evidenced by the two singlets at 23.6 and 22.6 ppm [14,26,27,46,47] in the ¹¹B NMR spectra (see Figure 2 for example, the representative ¹¹B NMR spectra for the interactions of the nickel complexes with HBcat under CO₂). The formation of CH₃OBcat was also confirmed by the singlet at 3.36 ppm [14,26,27,46] in the ¹H NMR spectra. Similar to the hydroboration of CO₂ with HBcat using the related nickel thiolato complexes as the catalysts [27], the ³¹P{¹H} NMR spectra were too complex to be understood—many unidentified species were shown. For complex **3a**, no reaction was observed after 60 min at temperatures up to 60 °C as evidenced by the ³¹P{¹H} NMR spectra. For complexes **1c**, **2c** and **3c**, black precipitate developed in 10 min and the ³¹P{¹H} NMR spectra showed that the original nickel complexes decomposed completely; neither CH₃OBcat nor catBOBcat were detected by the NMR spectra.

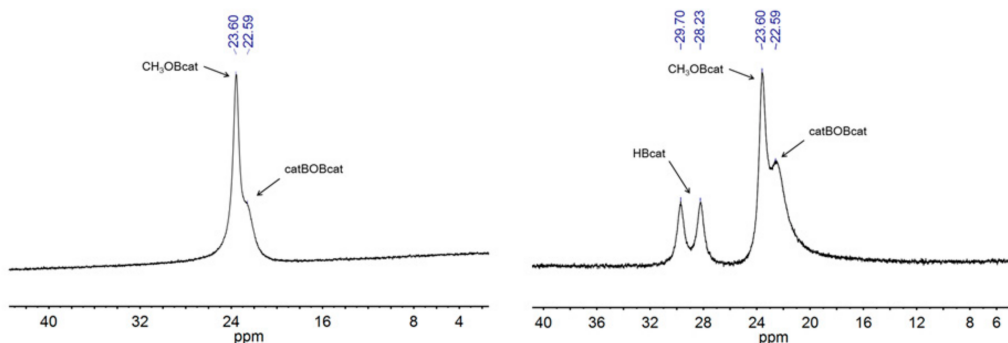
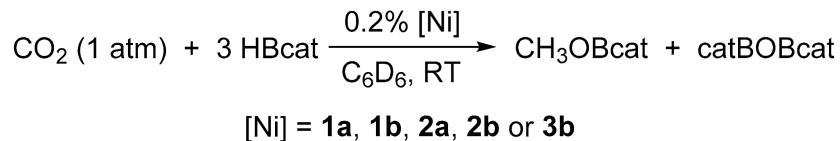


Figure 2. ¹¹B NMR spectra for the interactions of the nickel complexes (0.01 mmol) with HBcat (0.3 mmol) in benzene-*d*₆ (0.5 mL) under a CO₂ atmosphere at room temperature. The spectra were recorded 30 min after carbon dioxide was introduced into the NMR tube. (**left**, interaction of complex **1b** with HBcat; **right**, interaction of complex **3b** with HBcat).

The above NMR tube reactions indicate that complexes **1a**, **1b**, **2a**, **2b** and **3b** are active catalysts for the hydroboration of CO₂ with HBcat under mild conditions (Scheme 3).



Scheme 3. Catalytic hydroboration of CO₂ with HBcat.

Flask reactions were carried out to further evaluate the catalytic activities of these complexes. Typically, the nickel complex (0.01 mmol), HBcat (5 mmol) and C₆(CH₃)₆ (0.02 mmol, internal standard) were dissolved in benzene-*d*₆ (4 mL) under a nitrogen atmosphere. The solution was stirred at room temperature and CO₂ was bubbled through the solution at the same time. The reaction was stopped after a large amount of white precipitate developed. The reaction mixture was filtered and the clear liquid was analyzed by NMR spectroscopy. When complexes **3a** and **3b** were used as the catalysts, no white precipitate developed and the reaction was stopped after 2 h.

The isolated white precipitate was confirmed to be catBOBcat [14,26,27,46,47]. The ¹¹B NMR spectra of the clear reaction solutions indicated that HBcat was completely (for the reactions catalyzed **1a**, **1b**, **2a** or **2b**) or partly (for the reaction catalyzed by **3b**) converted to CH₃OBcat and catBOBcat. No product was detected for the reaction catalyzed by **3a**. Based on the ¹H NMR integrations of the CH₃OBcat methyl resonance (3.36 ppm) and the C₆(CH₃)₆ methyl resonance (2.11 ppm), turnover number (TON) was calculated for each of the reactions. Table 1 summarizes the results of the above catalytic reactions. A representative ¹H NMR spectrum of the clear reaction solution that was used to determine the TON value is shown in Figure 3.

Table 1. Turnover number (TON) and turnover frequency (TOF) obtained from the catalytic hydroboration of CO₂ with HBcat catalyzed by [2,6-(R₂PO)₂C₆H₃]NiX complexes ¹.

Catalyst	X	R	Time (min)	Conversion (%)	TON	TOF (h ⁻¹)
1a	SH	^t Bu	30	100	450 ± 19	900 ± 38
1b	SH	ⁱ Pr	15	100	465 ± 15	1860 ± 60
2a	N ₃	^t Bu	30	100	480 ± 11	960 ± 22
2b	N ₃	ⁱ Pr	15	100	477 ± 12	1908 ± 48
3a	NCS	^t Bu	120	0	0	0
3b	NCS	ⁱ Pr	120	68	325 ± 17	163 ± 9

¹ Conditions: 0.01 mmol of catalyst, 5.0 mmol of HBcat, 0.02 mmol of C₆(CH₃)₆ (internal standard); 4 mL of benzene-*d*₆, 1 atm of CO₂, room temperature; TONs (based on HBcat) were calculated from the ¹H NMR spectra and averaged from two to three independent experiments; conversions were based on the ¹¹B NMR spectra.

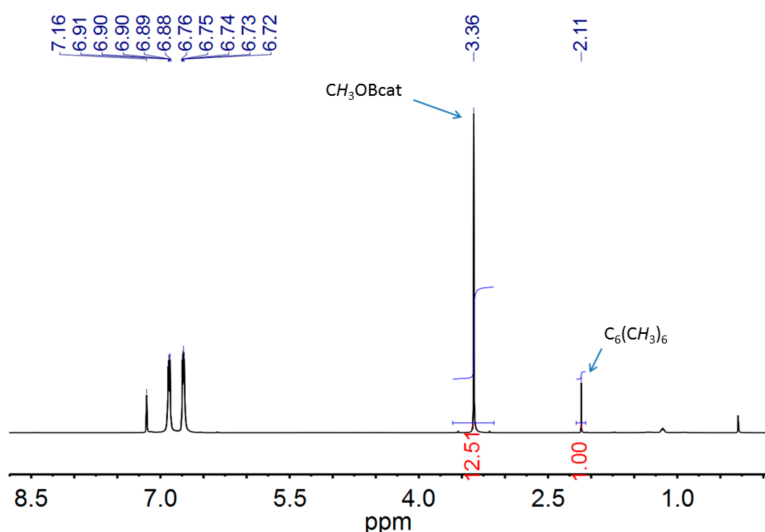


Figure 3. ^1H NMR spectrum for the hydroboration of CO_2 with HBcat catalyzed by complex **1a** in benzene- d_6 .

It can be seen from Table 1 that the mercapto and azido complexes have quite similar activities in catalyzing the hydroboration of CO_2 with HBcat and the catalytic activities are comparable to those of the corresponding palladium [26] and nickel [27] thiolato complexes reported previously. Complexes with isopropyl-substituted phosphine arms are more active than the corresponding complexes with *tert*-butyl substituted phosphine arms. This is in good agreement with the previous observation for the hydroboration of CO_2 with HBcat using the related nickel thiolato complexes as the catalysts [26,27]. Isothiocyanato complexes are far less active than the corresponding mercapto and azido complexes.

We previously reported that POCOP pincer ligated nickel mercapto complexes with $^t\text{Bu}_2\text{P}$ or $^i\text{Pr}_2\text{P}$ arms (**1a** and **1b**) can interact with HBcat at room temperature to generate POCOP pincer nickel hydride species [38]. In order to obtain more information, we checked the interactions of the other complexes (**1c**, **2a–c** and **3a–c**) with HBcat. The nickel complexes were treated with an excess amount of HBcat in C_6D_6 at room temperature in a sealed NMR tube and the reactions were monitored by NMR. For the interaction of **2a** or **2b** with HBcat, the hydride species $[2,6-(\text{R}_2\text{PO})_2\text{C}_6\text{H}_3]\text{NiH}$ [48] was detected by the $^{31}\text{P}\{^1\text{H}\}$ NMR spectra in 20 min. For the interaction of **3b** with HBcat, the hydride species was also observed in 2 h. However, no reaction was detected for the interaction of **3a** with HBcat after 24 h. When **1c**, **2c** or **3c** was treated with HBcat, black precipitate developed in 20 min and the original complex decomposed partly as evidenced by the $^{31}\text{P}\{^1\text{H}\}$ NMR spectra.

It should be noted that POCOP pincer nickel hydride species with entirely phenyl substituted phosphine arms cannot be synthesized because of the instability of this type of hydride complexes [48]. Therefore, the hydride species were not likely formed for the interaction of **1c**, **2c** or **3c** with HBcat.

The above experimental results are consistent with the speculation that these different types of pincer nickel complexes are pre-catalysts for the hydroboration of CO_2 with HBcat and the in situ generated pincer nickel hydrides are the actual active species to catalyze this reaction. Any POCOP pincer nickel complexes that can generate POCOP pincer nickel hydrides under the catalytic conditions are active catalysts for the hydroboration of CO_2 with catecholborane. The easier the hydride species can be generated, the more active the catalyst. For the hydroboration of carbon dioxide with HBcat using pure nickel hydrides as the catalysts, less bulky substituents on the phosphine arms make the catalysts less active because of the formation of an inactive complex outside the catalytic cycle [14–16]. However, for the hydroboration of CO_2 with HBcat using a pre-catalyst, such as POCOP pincer ligated nickel thiolato, mercapto, azido or isothiocyanato complex, the catalytic activity is also dependent on the ease or the difficulty to generate the active hydride species. Smaller substituents on the phosphine arms make it easier to generate the active hydride species, although other issues, such as the electronic

nature of the substituents on the phosphine arms [39,49,50] and the bond disassociation energy of the Ni–S or Ni–N bond [34,35], may also play important roles. On the other hand, the *in situ* generated other species, such as thiolato, azido and isothiosyanato species, may act as co-catalysts for this hydroboration reaction.

3. Materials and Methods

3.1. General Information

All manipulations were performed under an inert gas atmosphere. Solvents were degassed and dried before use. C₆D₆ was distilled from sodium and benzophenone before use. A Bruker Advance 400 MHz spectrometer (Swiss Bruker Corporation, Faellenan, Switzerland) was used for the NMR studies. For ¹H and ¹³C NMR spectra, the residual solvent resonances were used to calibrate the chemical shift values internally. For ³¹P and ¹¹B NMR spectra, H₃PO₄ (85%) and BF₃·Et₂O were used, respectively, to reference the chemical shift (δ) externally. Complexes [2,6-(Ph₂PO)₂C₆H₃]NiCl] [51], **1a** [37], **1b** [38], **2a–c** [35] and **3a–c** [35] were prepared as described in the literatures.

3.2. Synthesis of [2,6-(Ph₂PO)₂C₆H₃]NiSH (**1c**)

THF (10 mL) and MeOH (10 mL) were added to a flask containing [2,6-(Ph₂PO)₂C₆H₃]NiCl (572 mg, 1 mmol) and NaSH (280 mg, 5 mmol). The flask was then sealed and the resulting mixture in the flask was stirred at room temperature. After 48 h, the reaction was stopped and the volatiles were removed under vacuum. The residue was extracted with toluene and filtered through a pad of Celite. Complex **1c** was obtained as an orange solid (341 mg, 60% yield) after the solvent of the combined extractions were removed under vacuum. ¹H NMR (400 MHz, benzene-d₆, δ): 8.03–8.08 (m, 8H, ArH), 7.01 (t, 1H, ArH, $J_{\text{H-H}} = 6.9$ Hz), 6.94–7.00 (m, 12H, ArH), 6.83 (d, 2H, ArH, $J_{\text{H-H}} = 6.9$ Hz), –0.76 (t, 1H, SH, $J_{\text{H-P}} = 19.7$ Hz). ¹³C{¹H} NMR (101 MHz, benzene-d₆, δ): 167.0 (t, ArC, $J_{\text{C-P}} = 11.4$ Hz), 135.5 (s, ArC), 133.6 (t, ArC, $J_{\text{C-P}} = 24.0$ Hz), 132.6 (t, ArC, $J_{\text{C-P}} = 7.2$ Hz), 131.6 (s, ArC), 129.6 (s, ArC), 128.9 (t, ArC, $J_{\text{C-P}} = 5.8$ Hz), 106.7 (t, ArC, $J_{\text{C-P}} = 7.2$ Hz). ³¹P{¹H} NMR (162 MHz, benzene-d₆, δ): 152.9 (s). Selected data from FTIR (KBr disc, cm^{−1}): 2546 (w), 1435 (s), 1106 (m), 838 (s). Anal. Calcd for C₃₀H₂₄NiO₂P₂S: C, 63.30; H, 4.25. Found: C, 63.07; H, 4.11.

3.3. X-ray Structure Determination of [2,6-(Ph₂PO)₂C₆H₃]NiSH (**1c**)

Single crystals of **1c** used for X-ray diffraction analysis were obtained from *n*-hexane/CH₂Cl₂ solution at –10 °C. The identities of the resulting crystals were confirmed by ³¹P{¹H} NMR spectroscopy before the X-ray diffraction analysis. The intensity data were collected at 103 K on a Bruker SMART6000 CCD diffractometer. A graphite-monochromated Mo K α radiation ($\lambda = 0.71073$ Å) was used for the data collection. Details for the data processing and structure refinement were similar to our previously reported procedures [37]. A summary of crystallographic data and structure refinement for complex **1c** is provided in Table 2.

CCDC 1869263 contains the supplementary crystallographic data for complex **1c**. These data can be obtained free of charge from The Cambridge Crystallographic Data Centre (The Cambridge Structural Database, Cambridge, UK).

3.4. Procedure for the Catalytic Hydroboration of CO₂

Flask experiments for the catalytic hydroboration of carbon dioxide were carried out at room temperature under an atmospheric pressure of carbon dioxide in benzene-d₆ with a catalyst-to-substrate ratio of 1:500. The nickel catalyst (0.01 mmol), HBcat (5.00 mmol), hexamethylbenzene (0.02 mmol) and benzene-d₆ (4 mL) were mixed in a flame-dried 50 mL Schlenk flask under N₂. Then CO₂ was bubbled through the solution until a large amount of white precipitate developed. The mixture was stirred for an additional 2 min. The resulting white precipitate was then allowed to settle, and 0.6 mL of the clear liquid was transferred under nitrogen into a NMR tube. ¹¹B and ¹H NMR spectra were

then recorded. The TON numbers were calculated based on the ^1H NMR integrations of the CH_3OBcat methyl resonance at 3.36 ppm and the $\text{C}_6(\text{CH}_3)_6$ (internal standard) methyl resonance at 2.11 ppm. The conversions were calculated from the ^{11}B NMR spectra.

Table 2. Summary of crystal data and structure refinement for complex **1c**.

Empirical formula	$\text{C}_{30}\text{H}_{24}\text{NiO}_2\text{P}_2\text{S}$	Volume, \AA^3	2582.0(3)
Formula weight	569.20	Z	4
Temp, K	103(2)	d_{calc} , g cm^{-3}	1.464
Crystal system	Monoclinic	λ , \AA	0.71073
Space group	P 1 21/c 1	μ , mm^{-1}	0.983
a , \AA	14.9995(10)	No. of data collected	29,194
b , \AA	9.9798(5)	No. of unique data	10,374
c , \AA	17.2488(12)	R_{int}	0.0895
α ($^\circ$)	90	Goodness-of-fit on F^2	1.003
β ($^\circ$)	90.195(3)	R_1 , wR_2 ($I > 2\sigma(I)$)	0.0583, 0.1182
γ ($^\circ$)	90	R_1 , wR_2 (all data)	0.1111, 0.1411

4. Conclusions

In summary, we have applied three different types of POCOP pincer nickel complexes (i.e., mercapto complex, azido complex and isothiosyanato complex) to the catalytic hydroboration of carbon dioxide with catecholborane. CO_2 was successfully reduced to a methanol derivative (CH_3OBcat) under an atmospheric pressure of CO_2 at room temperature with TOFs up to 1908 h^{-1} . It was found that pincer complexes with isopropyl-substituted phosphine arms are more active than the corresponding complexes with *tert*-butyl substituted phosphine arms. Complexes with phenyl-substituted phosphine arms decomposed under the catalytic conditions and failed to catalyze the reactions. Of the three types of complexes, the isothiosyanato complex is far less active than the corresponding mercapto and azido complexes. It is concluded that all of these catalytically active complexes are catalyst precursors which generate the nickel hydride complex $[2,6-(\text{R}_2\text{PO})_2\text{C}_6\text{H}_3]\text{NiH}$ *in situ* under the catalytic conditions, and the nickel hydride complex is the active species to catalyze this reaction.

Author Contributions: Conceptualization, J.Z.; Methodology, J.Z.; Validation, J.Z. and X.C.; Investigation, J.C., T.L., B.C. and Y.D.; Resources, J.Z. and X.C.; Data curation, X.C.; Writing—Original Draft Preparation, J.C., T.L. and B.C.; Writing—Review and Editing, J.Z.; Visualization, J.Z.; Supervision, J.Z. and X.C.; Project Administration, J.Z. and X.C.; Funding Acquisition, J.Z. and X.C.

Funding: This research was funded by the National Natural Science Foundation of China, grant numbers 21571052 and 21771057.

Conflicts of Interest: The authors declare no conflict of interest. The funder had no role in the design of the study; in the collection, analyses, or interpretation of data; in the writing of the manuscript, or in the decision to publish the results.

References

- Kortlever, R.; Shen, J.; Schouten, K.J.P.; Calle-Vallejo, F.; Koper, M.T.M. Catalysts and reaction pathways for the electrochemical reduction of carbon dioxide. *J. Phys. Chem. Lett.* **2015**, *6*, 4073–4082. [[CrossRef](#)] [[PubMed](#)]
- Costentin, C.; Roberta, M.; Savéant, J.-M. Catalysis of the electrochemical reduction of carbon dioxide. *Chem. Soc. Rev.* **2013**, *42*, 2423–2436. [[CrossRef](#)] [[PubMed](#)]
- Takeda, H.; Ishitani, O. Development of efficient photocatalytic systems for CO_2 reduction using mononuclear and multinuclear metal complexes based on mechanistic studies. *Coord. Chem. Rev.* **2010**, *254*, 346–354. [[CrossRef](#)]
- Chong, C.C.; Kirjo, R. Catalytic hydroboration of carbonyl derivatives, imines, and carbon dioxide. *ACS Catal.* **2015**, *5*, 3238–3259. [[CrossRef](#)]
- Benson, E.E.; Kubiak, C.P.; Sathrum, A.J.; Smieja, J.M. Electrocatalytic and homogeneous approaches to conversion of CO_2 to liquid fuels. *Chem. Soc. Rev.* **2009**, *38*, 89–99. [[CrossRef](#)] [[PubMed](#)]

6. Wang, W.-H.; Himeda, Y.; Muckerman, J.T.; Manbeck, G.F.; Fujita, E. CO₂ hydrogenation to formate and methanol as an alternative to photo- and electrochemical CO₂ reduction. *Chem. Rev.* **2015**, *115*, 12936–12973. [[CrossRef](#)] [[PubMed](#)]
7. Ali, K.A.; Abdullah, A.Z.; Mohamed, A.R. Recent development in catalytic technologies for methanol synthesis from renewable sources: A critical review. *Renew. Sustain. Energy Rev.* **2015**, *44*, 508–518. [[CrossRef](#)]
8. Ganesh, I. Conversion of carbon dioxide into methanol—A potential liquid fuel: Fundamental challenges and opportunities (a review). *Renew. Sustain. Energy Rev.* **2014**, *31*, 221–257. [[CrossRef](#)]
9. Fontaine, F.-G.; Courtemanche, M.-A.; Légaré, M.-A. Transition-metal-free catalytic reduction of carbon dioxide. *Chem. Eur. J.* **2014**, *20*, 2990–2996. [[CrossRef](#)] [[PubMed](#)]
10. Habirreu-tinger, S.N.; Schmidt-Mende, L.; Stolarczyk, J.K. Photocatalytic reduction of CO₂ on TiO₂ and other semiconductors. *Angew. Chem. Int. Ed.* **2013**, *52*, 7372–7408. [[CrossRef](#)] [[PubMed](#)]
11. Appel, A.M.; Bercaw, J.E.; Bocarsly, A.B.; Dobbek, H.; DuBois, D.L.; Dupuis, M.; Ferry, J.G.; Fujita, E.; Hille, R.; Kenis, P.J.A. Frontiers, opportunities, and challenges in biochemical and chemical catalysis of CO₂ fixation. *Chem. Rev.* **2013**, *113*, 6621–6658. [[CrossRef](#)] [[PubMed](#)]
12. Aresta, M.; Dibenedetto, A.; Angelini, A. Catalysis for the valorization of exhaust carbon: From CO₂ to chemicals, materials, and fuels. Technological use of CO₂. *Chem. Rev.* **2014**, *114*, 1709–1742. [[CrossRef](#)] [[PubMed](#)]
13. Arakawa, H.; Aresta, M.; Armor, J.N.; Barreau, M.A.; Beckman, E.J.; Bell, A.T.; Bercaw, J.E.; Creutz, C.; Dinjus, E.; Dixon, D.A.; et al. Catalysis research of relevance to carbon management: Progress, challenges, and opportunities. *Chem. Rev.* **2001**, *101*, 953–996. [[CrossRef](#)] [[PubMed](#)]
14. Chakraborty, S.; Zhang, J.; Krause, J.A.; Guan, H. An efficient nickel catalyst for the reduction of carbon dioxide with a borane. *J. Am. Chem. Soc.* **2010**, *132*, 8872–8873. [[CrossRef](#)] [[PubMed](#)]
15. Chakraborty, S.; Zhang, J.; Patel, Y.J.; Krause, J.A.; Guan, H. Pincer-ligated nickel hydridoborate complexes: The dormant species in catalytic reduction of carbon dioxide with boranes. *Inorg. Chem.* **2013**, *52*, 37–47. [[CrossRef](#)] [[PubMed](#)]
16. Chakraborty, S.; Patel, Y.J.; Krause, J.A.; Guan, H. Catalytic properties of nickel bis(phosphinite) pincer complexes in the reduction of CO₂ to methanol derivatives. *Polyhedron* **2012**, *32*, 30–34. [[CrossRef](#)]
17. Wesselbaum, S.; vom Stein, T.; Klankermayer, J.; Leitner, W. Hydrogenation of carbon dioxide to methanol by using a homogeneous ruthenium–phosphine catalyst. *Angew. Chem. Int. Ed.* **2012**, *51*, 7499–7502. [[CrossRef](#)] [[PubMed](#)]
18. Huff, C.A.; Sanford, M.S. Cascade catalysis for the homogeneous hydrogenation of CO₂ to methanol. *J. Am. Chem. Soc.* **2011**, *133*, 18122–18125. [[CrossRef](#)] [[PubMed](#)]
19. Rezayee, N.M.; Huff, C.A.; Sanford, M.S. Tandem amine and ruthenium-catalyzed hydrogenation of CO₂ to methanol. *J. Am. Chem. Soc.* **2015**, *137*, 1028–1031. [[CrossRef](#)] [[PubMed](#)]
20. Tominaga, K.; Sasaki, Y.; Kawai, M.; Watanabe, T.; Saito, M. Ruthenium complex catalysed hydrogenation of carbon dioxide to carbon monoxide, methanol and methane. *J. Chem. Soc. Chem. Commun.* **1993**, *0*, 629–631. [[CrossRef](#)]
21. Wesselbaum, S.; Moha, V.; Meuresch, M.; Brosinski, S.; Thenert, K.M.; Kothe, J.; vom Stein, T.; Englert, U.; Hölscher, M.; Klankermayer, J.; et al. Hydrogenation of carbon dioxide to methanol using a homogeneous ruthenium–triphos catalyst: From mechanistic investigations to multiphase catalysis. *Chem. Sci.* **2015**, *6*, 693–704. [[CrossRef](#)] [[PubMed](#)]
22. Kothandaraman, J.; Goeppert, A.; Czaun, M.; Olah, G.A.; Prakash, G.K.S. Conversion of CO₂ from air into methanol using a polyamine and a homogeneous ruthenium catalyst. *J. Am. Chem. Soc.* **2016**, *138*, 778–781. [[CrossRef](#)] [[PubMed](#)]
23. Lu, Z.; Williams, T.J. Di(carbene)-supported nickel systems for CO₂ reduction under ambient conditions. *ACS Catal.* **2016**, *6*, 6670–6673. [[CrossRef](#)]
24. Bontemps, S.; Vendier, L.; Sabo-Etienne, S. Borane-mediated carbon dioxide reduction at ruthenium: Formation of C1 and C2 compounds. *Angew. Chem. Int. Ed.* **2012**, *51*, 1671–1674. [[CrossRef](#)] [[PubMed](#)]
25. Hadlington, T.J.; Kefalidis, C.E.; Maron, L.; Jones, C. Efficient reduction of carbon dioxide to methanol equivalents catalyzed by two-coordinate amido–germanium(II) and–tin(II) hydride complexes. *ACS Catal.* **2017**, *7*, 1853–1859. [[CrossRef](#)]

26. Ma, Q.-Q.; Liu, T.; Li, S.; Zhang, J.; Chen, X.; Guan, H. Highly efficient reduction of carbon dioxide with a borane catalyzed by bis(phosphinite) pincer ligated palladium thiolate complexes. *Chem. Commun.* **2016**, *52*, 14262–14265. [[CrossRef](#)] [[PubMed](#)]
27. Liu, T.; Meng, W.; Ma, Q.-Q.; Zhang, J.; Li, H.; Li, S.; Zhao, Q.; Chen, X. Hydroboration of CO₂ catalyzed by bis(phosphinite) pincer ligated nickel thiolate complexes. *Dalton Trans.* **2017**, *46*, 4504–4509. [[CrossRef](#)] [[PubMed](#)]
28. Tamang, S.R.; Findlater, M. Cobalt catalysed reduction of CO₂ via hydroboration. *Dalton Trans.* **2018**, *47*, 8199–8203. [[CrossRef](#)] [[PubMed](#)]
29. Li, H.; Gonçalves, T.P.; Zhao, Q.; Gong, D.; Lai, Z.; Wang, Z.; Zheng, J.; Huang, K.-W. Diverse catalytic reactivity of a dearomatized PN³P*-nickel hydride pincer complex towards CO₂ reduction. *Chem. Commun.* **2018**, *54*, 11395–11398. [[CrossRef](#)] [[PubMed](#)]
30. Yu, D.-G.; Li, B.-J.; Shi, Z.-J. Exploration of new C–O electrophiles in cross-coupling reactions. *Acc. Chem. Res.* **2010**, *43*, 1486–1495. [[CrossRef](#)] [[PubMed](#)]
31. Tasker, S.Z.; Standley, E.A.; Jamison, T.F. Recent advances in homogeneous nickel catalysis. *Nature* **2014**, *509*, 299–309. [[CrossRef](#)] [[PubMed](#)]
32. Su, B.; Cao, Z.-C.; Shi, Z.-J. Exploration of earth-abundant transition metals (Fe, Co, and Ni) as catalysts in unreactive chemical bond activations. *Acc. Chem. Res.* **2015**, *48*, 886–896. [[CrossRef](#)] [[PubMed](#)]
33. Zhang, J.; Medley, C.M.; Krause, J.A.; Guan, H. Mechanistic insights into C–S cross-coupling reactions catalyzed by nickel bis(phosphinite) pincer complexes. *Organometallics* **2010**, *29*, 6393–6401. [[CrossRef](#)]
34. Zhang, J.; Adhikary, A.; King, K.M.; Krause, J.A.; Guan, H. Substituent effects on Ni–S bond dissociation energies and kinetic stability of nickel arylthiolate complexes supported by a bis(phosphinite)-based pincer ligand. *Dalton Trans.* **2012**, *41*, 7959–7968. [[CrossRef](#)] [[PubMed](#)]
35. Li, H.; Meng, W.; Adhikary, A.; Li, S.; Ma, N.; Zhao, Q.; Yang, Q.; Eberhardt, N.A.; Leahy, K.M.; Krause, J.A.; et al. Metathesis reactivity of bis(phosphinite) pincer ligated nickel chloride, isothiocyanate and azide complexes. *J. Organomet. Chem.* **2016**, *804*, 132–141. [[CrossRef](#)]
36. Ma, Q.-Q.; Liu, T.; Adhikary, A.; Zhang, J.; Krause, J.A.; Guan, H. Using CS₂ to probe the mechanistic details of decarboxylation of bis(phosphinite)-ligated nickel pincer formate complexes. *Organometallics* **2016**, *35*, 4077–4082. [[CrossRef](#)]
37. Zhang, J.; Liu, T.; Ma, Q.-Q.; Li, S.; Chen, X. A reaction of [2,6-(^tBu₂PO)₂C₆H₃]NiSCH₂Ph with BH₃·THF: Borane mediated C–S bond cleavage. *Dalton Trans.* **2018**, *47*, 6018–6024. [[CrossRef](#)] [[PubMed](#)]
38. Zhang, J.; Liu, T.; Wei, C.; Chang, J.; Ma, Q.-Q.; Li, S.; Ma, N.; Chen, X. The reactivity of mercapto groups against boron hydrides in pincer ligated nickel mercapto complexes. *Chem. Asian J.* **2018**, *13*. [[CrossRef](#)] [[PubMed](#)]
39. Vabre, B.; Spasyuk, M.D.; Zargarian, D. Impact of backbone substituents on POCOP-Ni pincer complexes: A structural, spectroscopic, and electrochemical study. *Organometallics* **2012**, *31*, 8561–8570. [[CrossRef](#)]
40. Vabre, B.; Petiot, P.; Declercq, R.; Zargarian, D. Fluoro and trifluoromethyl derivatives of POCOP-type pincer complexes of nickel: Preparation and reactivities in S_N2 fluorination and direct benzylation of unactivated arenes. *Organometallics* **2014**, *33*, 5173–5184. [[CrossRef](#)]
41. Hao, J.; Vabre, B.; Zargarian, D. POCOP-ligated nickel siloxide complexes: Syntheses, characterization, and reactivities. *Organometallics* **2014**, *33*, 6568–6576. [[CrossRef](#)]
42. Lapointe, S.; Vabre, B.; Zargarian, D. POCOP-type pincer complexes of nickel: Synthesis, characterization, and ligand exchange reactivities of new cationic acetonitrile adducts. *Organometallics* **2015**, *34*, 3520–3531. [[CrossRef](#)]
43. Buil, M.L.; Elipe, S.; Esteruelas, M.A.; Oñate, E.; Peinado, E.; Ruiz, N. Five-coordinate complexes MHCl(CO)(PⁱPr₃)₂ (M = Os, Ru) as precursors for the preparation of new hydrido- and alkenyl-metallothiol and monothio-β-diketonato derivatives. *Organometallics* **1997**, *16*, 5748–5755. [[CrossRef](#)]
44. Vicic, D.A.; Jones, W.D. Room-temperature desulfurization of dibenzothiophene mediated by [(i-Pr₂PCH₂)₂NiH]₂. *J. Am. Chem. Soc.* **1997**, *119*, 10855–10856. [[CrossRef](#)]
45. Di Vaira, M.; Peruzzini, M.; Stoppioni, P. Hydrochalcogenide and hydride hydrochalcogenide derivatives of rhodium. *Inorg. Chem.* **1991**, *30*, 1001–1007. [[CrossRef](#)]
46. Courtemanche, M.A.; Legare, M.A.; Maron, L.; Fontaine, F.G. A highly active phosphine–borane organocatalyst for the reduction of CO₂ to methanol using hydroboranes. *J. Am. Chem. Soc.* **2013**, *135*, 9326–9329. [[CrossRef](#)] [[PubMed](#)]

47. Lang, A.; Knizek, J.; Nöth, H.; Schur, S.; Thomann, M. Beiträge zur chemie des bors. 237. Bis(benzo-1,3,2-dioxaborolanyl)oxid und 2-(o-hydroxyphenoxy)-benzo-1,3,2-dioxaborolan. Vorstufen zur synthese von catecholboran (benzo-1,3,2-dioxaborolan). *Z. Anorg. Allg. Chem.* **1997**, *623*, 901–907. [[CrossRef](#)]
48. Chakraborty, S.; Krause, J.A.; Guan, H. Hydrosilylation of aldehydes and ketones catalyzed by nickel PCP-pincer hydride complexes. *Organometallics* **2009**, *28*, 582–586. [[CrossRef](#)]
49. Castonguay, A.; Spasyuk, D.M.; Madern, N.; Beauchamp, A.L.; Zargarian, D. Regioselective hydroamination of acrylonitrile catalyzed by cationic pincer complexes of Nickel(II). *Organometallics* **2009**, *28*, 2134–2141. [[CrossRef](#)]
50. Salah, A.B.; Zargarian, D. The impact of P-substituents on the structures, spectroscopic properties, and reactivities of POCOP-type pincer complexes of Nickel(II). *Dalton Trans.* **2011**, *40*, 8977–8985. [[CrossRef](#)] [[PubMed](#)]
51. Gómez-Benítez, V.; Baldovino-Pantaleón, O.; Herrera-Álvarez, C.; Toscano, R.A.; Morales-Morales, D. High yield thiolation of iodobenzene catalyzed by the phosphinite nickel PCP pincer complex: $[\text{NiCl}(\text{C}_6\text{H}_3\text{-}2,6\text{-(OPPh}_2)_2)]$. *Tetrahedron Lett.* **2006**, *47*, 5059–5062. [[CrossRef](#)]



© 2018 by the authors. Licensee MDPI, Basel, Switzerland. This article is an open access article distributed under the terms and conditions of the Creative Commons Attribution (CC BY) license (<http://creativecommons.org/licenses/by/4.0/>).